2016

Si-containing precursors for Si-based anode materials of Li-ion batteries: A review

Lei Zhang
University of Wollongong, Huazhong University of Science and Technology,, lz755@uowmail.edu.au

Xiaoxiao Liu
Huazhong University of Science and Technology

Qianjin Zhao
Huazhong University of Science and Technology

Shi Xue Dou
University of Wollongong, shi@uow.edu.au

Hua-Kun Liu
University of Wollongong, hua@uow.edu.au

See next page for additional authors

Publication Details

Zhang, L., Liu, X., Zhao, Q., Dou, S., Liu, H., Huang, Y. & Hu, X. (2016). Si-containing precursors for Si-based anode materials of Li-ion batteries: A review. Energy Storage Materials, 4 92-102.

Si-containing precursors for Si-based anode materials of Li-ion batteries: A review

Abstract
Lithium-ion batteries with high energy density are in demand for consumer electronics, electric vehicles, and grid-scale stationary energy storage. Si is one of the most promising anode materials due to its extremely high specific capacity. However, the full application of Si-based anode materials is limited by poor cycle life and rate capability resulted from low ionic/electronic conductivity and large volume change over cycling. In recent years, great progress has been made in improving the performance of Si anodes by employing nanotechnology. The preparation methods are essentially important, in which the precursors used are crucial to design and control the microstructure for the Si-based materials. In this review, we provide comprehensive summary and comment on different Si-containing precursors for preparation of nanosized Si-based anode materials and focus on the corresponding electrochemical performances in lithium-ion batteries. Bulk sized silicon, silicon wafer and silicon microparticles are generally used as starting materials to synthesize porous or nanosized silicon, and the routes for the synthesis are rather mature and commercially available. Silica is also commonly used to form silicon by conversion through a facile magnesiothermic reduction. Silica derivation from natural resources, especially from rice husks, is much more sustainable and lower cost than alternative methods, which attracts considerable research attention. In addition, gaseous Si-based sources like SiH4, Si2H6 and SiHxCly, liquid silicon sources like trisilane and phenylsilane and elemental silicon have successfully used to prepare nanosized or carbon-coated silicon. Further considerations on massive production possibility have also been presented.

Keywords
batteries, anode, precursors, li, containing, review, si, materials, ion

Disciplines
Engineering | Physical Sciences and Mathematics

Publication Details
Zhang, L., Liu, X., Zhao, Q., Dou, S., Liu, H., Huang, Y. & Hu, X. (2016). Si-containing precursors for Si-based anode materials of Li-ion batteries: A review. Energy Storage Materials, 4 92-102.

Authors
Lei Zhang, Xiaoxiao Liu, Qianjin Zhao, Shi Xue Dou, Hua-Kun Liu, Yunhui Huang, and Xianluo Hu

Si-Containing Precursors for Si-Based Anode Materials of Li-Ion Batteries

Lei Zhang,[ab] Xiaoxiao Liu,[a] Qianjin Zhao,[a] Shixue Dou,[b] Huakun Liu,[b*] Yunhui Huang,[a*] and Xianluo Hu[a*]

a. State Key Laboratory of Material Processing and Die & Mould Technology, School of Materials Science and Engineering, Huazhong University of Science and Technology, Wuhan 430074, China.

b. Institute for Superconducting and Electronic Materials, University of Wollongong, Wollongong, NSW 2522, Australia.

*To whom correspondence should be addressed. E-mail addresses: hua@uow.edu.au (H. Liu), huangyh@hust.edu.cn (Yunhui Huang), and huxl@hust.edu.cn (Xianluo Hu).

Abstract

Lithium-ion batteries with high energy density and large power output are in demand for consumer electronics, electric vehicles, and grid-scale stationary energy storage. Silicon is one of the most promising anode materials because it has 10 times higher specific capacity than that of the commercial graphitic carbon anode. Unfortunately, the practical utilization of silicon-based anode materials is still hindered by its low electronic conductivity and high capacity fading rate due to the large volume changes upon insertion and extraction of Li ions during cycling. Introducing porous structure, along with decreasing the dimension of Si-based materials to nanosize, is an effective way to address these problems. During the past decade, tremendous attention has been paid to improve Si anodes so as to give them better electrochemical performance. In this review, we focus the Si-containing precursors for preparation of Si-based anode materials.

1. Introduction

With more engines up and running, sustainable development for the entire human race will be at risk. The burning of fuels results in global warming and air pollution by giving off all kinds of exhaust gases. Therefore, producing energy from renewable and sustainable resources is preferable. Rechargeable batteries are in demand for consumer electronics, electric vehicles, and grid-scale stationary energy storage because the technology is feasible, environmentally friendly, and sustainable.[1-6] Among the different kinds of rechargeable batteries, lithium-ion batteries (LIBs) are the most popular ones, due to their high energy density, lack of any memory effect, and only a slow loss of capacity when not in use.[7,8] The traditional commercial anode materials for LIBs, such as graphite microspheres (GMs) and mesophase carbon microbeads (MCMBs), however, have relatively low capacity (only 372 mA h g^{-1}, corresponding to a fully lithiated state of LiC_6), so that they are not suitable for future LIBs with high energy density and large power output.[9-11]

To further increase the energy density of LIBs for the above-mentioned applications, alloy-type anodes such as Si, Ge, and Sn have been extensively explored because of their high capacity.[12-21] Among them, Si is a promising candidate to replace the traditional graphite anode for high-capacity LIBs, since it has 10 times (～4200 mA h g^{-1}) higher specific capacity through forming the alloy $Li_{22}Si_5$.[22-24] Compared with other alloy-type and metal oxide anodes, the discharging potential of silicon (～0.2 V against Li/Li^+) is lower, leading to a higher energy density for full cells. Furthermore, its appealing characteristics, such as abundance and environmental benignity, make silicon the most attractive anode material for LIBs.[25]

Despite all of these advantages, the full utilization of silicon-based LIBs to date has been hindered by a series of obstacles, including poor cycle life and rate performance, that result from its low ionic/electronic conductivity and large volume changes during the lithium insertion and

extraction processes.[26-28] When silicon is fully lithiated, the equilibrium Li-Si alloy with the highest Li concentration is the $Li_{22}Si_5$ phase, which causes dramatic structural changes (about 400% volume expansion).[22] The volumetric and structural changes can result in the pulverization of the initial particles, which means that the silicon can no longer hold Li^+ ions effectively, and the bulk silicon experiences a rapid decay of the specific capacity.[24] Moreover, when the silicon expands and contracts, the solid-electrolyte interphase (SEI) film on the outer surface of the electrode will also break up in a cyclical manner, resulting in the continual formation of new SEI films.[18]

In the past decade, tremendous attention has been paid to improving the electrochemical performance of Si-based anodes by designing and fabricating new and different silicon structures, particularly in the nanosized range.[29] Compared with the microsized Si-based materials, the nanomaterials are endowed with several advantages: (1) the high surface-to-volume ratio of nanomaterials can better withstand stress and limit the cracking caused by the volume expansion during cycling, thus maintaining high specific capacity with improved cycling stability; and (2) the nanosized particles can provide stable electronic and ionic transfer channels to shorten the diffusion length of Li^+ species, resulting in an increased rate capability and reduced polarization. Apart from the nanostructured silicon, porous Si-based compounds are also promising for practical applications, because the newly created void space can accommodate the volume changes during the charge–discharge processes, enhancing the structural and cycling stability.

In this review article, we aim to provide a comprehensive summary focusing on the preparation of Si-based anodes in the nanosize regime from different precursors, in contrast to some previous review articles on a similar topic.

2. Si-containing precursors for nanosized or porous Si anode materials

2.1 Bulk sized silicon

As the second most abundant element in the earth, silicon has great potential to be employed as a LIB anode at a very low cost. The bulk-sized Si materials, such as Si wafers and microsized Si particles, are frequently employed as starting materials to synthesize porous or nanosized silicon via a top-down approach. The routes for the synthesis of silicon nanoparticles (SiNPs) from bulk silicon are rather mature and commercially available, which means that SiNPs are compatible with the traditional manufacturing process for commercial LIB electrodes.

2.1.1 Silicon wafer

Facile methods such as electroless etching[30-41] and electrochemical etching[42-48] are able to convert bulk silicon wafer into a porous structure with tunable pore size and porosity, which is called 'integral' porosity. For example, with an appropriately doped Si wafer, porous Si and Si nanowires can be synthesized in the presence of silver nitrate ($AgNO_3$) in hydrofluoric acid (HF) etchant solution.[49,50] Typically, there are two reactions taking place:

$$4Ag^+ + 4e^- \rightarrow 4Ag \quad (1)$$

$$Si + 6F^- \rightarrow [SiF_6]^{2-} + 4e^- \quad (2)$$

During this reaction, nanosized silicon with a porous or wire-like structure can be synthesized by localized catalytic etching of the Si wafer in HF solution.[51,52] The galvanic displacement reaction between Ag^+ ions and Si can create Ag clusters and SiO_x simultaneously. SiO_x is at the bottom of the Ag clusters and can be easily dissolved by HF, leading to the production of nanocups right under the Ag clusters. The formation and subsequent dissolution of SiO_x can proceed continuously, due to the further deposition of Ag, thus further "digging" the holes in the Si substrate underneath the Ag particles,[52] resulting an array of Si nanowires. For example, large-area, oriented Si nanowire arrays formed on the Si wafer at near room temperature by localized chemical etching were reported by Zhu's group (Figure 1a and 1b).[53] This strategy is based on Ag-induced excessive local

oxidation and dissolution of a silicon substrate in an HF solution. It was found that the distribution of Ag clusters on the Si wafer surface to be patterned by Ag particles has a great effect on the size and density of the thus-prepared silicon nanowires. High-density metal particles can facilitate the formation of Si nanowires, and a larger space among the Ag clusters can lead to better-separated nanoholes in the Si wafer. In addition, porous silicon with a large pore size and high porosity was prepared by Zhou[54] via this electroless etching method using the silicon wafer as the Si precursor (Figure 1c). In this work, porous Si nanowires were produced by direct etching of boron-doped Si wafers and exhibited superior electrochemical performance and long cycle life as the anode material in a LIB, using alginate as the binder. As reported, the capacity remained stable above 2000, 1600, and 1100 mAh g^{-1} at current densities of 2, 4, and 18 A g^{-1}, respectively, even after 250 cycles. The good cycling stability mainly stems from the use of a porous silicon structure, while the use of a commercial alginate binder also helped to a certain degree as compared to the commonly used polyvinylidene fluoride (PVDF).[54]

Silicon wafer is also a precursor for fabrication of porous silicon via an electrochemical etching method which was first accidentally discovered by Uhlir at Bell Laboratories in the 1950s.[55,56] The porous Si electrode can be produced via electrochemical etching on a silicon wafer using a HF etching solution and a constant current density.[57] The porosity and depth of the porous silicon can be adjusted by the current density and HF concentration.[56] Based on this technique, Sibani Lisa Biswal[58] presented a layered architecture consisting of a gold-coated porous silicon film attached to a bulk silicon substrate (Figure 1d). It was found that a specific capacity of more than 3000 mAh g^{-1} can be achieved for 50 cycles at 100 μA cm^{-2}, and 2500 mAh g^{-1} can be achieved for 75 cycles with coulombic efficiency of >95%.

For summary, uniform distribution can be obtained either for the silicon nanowires or the porous structure. And the size of these wires and pores are both in a range of nanosized distribution.

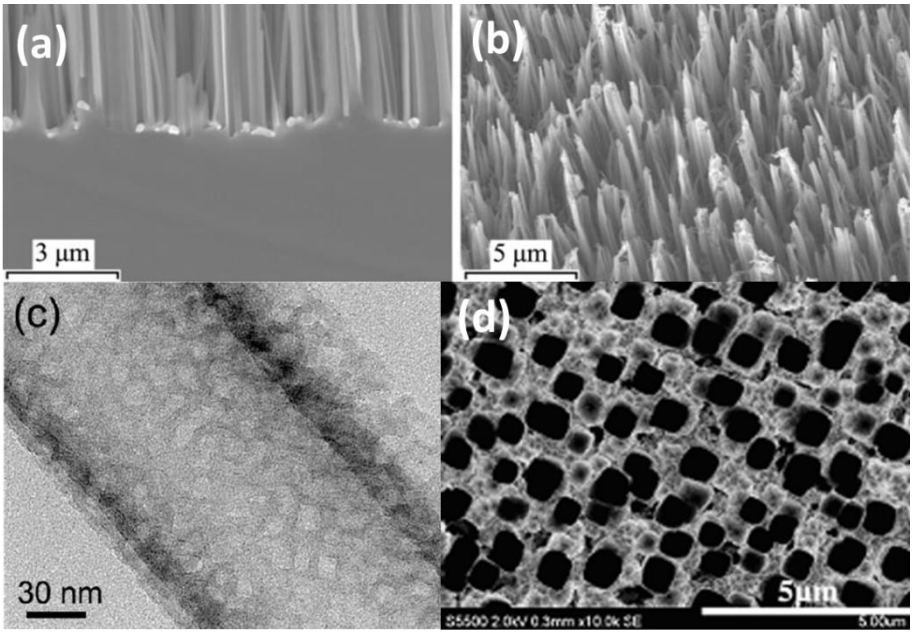

Figure 1. (a) Scanning electron microscope (SEM) cross-sectional image of the as-synthesized silicon wires arrays shown in (b).[53] Copyright 2006, Wiley-VCH Verlag GmbH and Co. KGaA, Weinheim. (c) high resolution transmission electron microscope (HRTEM) image of a single nanowire,[54] Copyright 2012, American Chemical Society; and (d) top-view SEM image of a representative porous silicon sample.[58] Copyright 2012, Elsevier.

2.1.2 Silicon microparticles

Apart from the silicon wafer, microsized Si particles can also be employed as the silicon precursor to prepare porous silicon via an electroless etching process. Compared with silicon wafer, microsized silicon is much cheaper and easily-accessed, which makes it more available for scalable production. Nevertheless, it is a great challenge to produce structure-regulated silicon nanowires from silicon microparticles because of their irregular morphology and crystallization characteristics. Therefore, in recent research, microsized silicon powders have always been employed as the silicon precursor to prepare porous silicon through various modified electroless etching methods. For

example, Su's group employed commercial metallurgical-grade silicon particles as the primary silicon source through a modified ferrite (Fe)-assisted chemical etching method to prepare porous silicon particles (Figure 2a and 2b).[59] In this reaction, porous silicon particles were produced through a reaction between Fe and silicon in the surrounding glycol. Taking advantages of the porous structure, the anodes made from these silicon bulks exhibit high reversible capacity and long cycle life. In addition, Su's group also used commercial silicon microparticles as the silicon source to react with CH_3Cl gas over a Cu-based catalyst to create large amounts of macropores within the unreacted silicon (Figure 2c and 2d).[40] Thanks to the interconnected porous structure, this porous silicon-based anode material exhibited excellent electrochemical performance. The discharge capacity of this silicon-based porous material was around 1000 mAh g^{-1} after 100 cycles, and the average capacity fading rate of this anode was around 0.35%/cycle. Meanwhile, it also showed very good rate performance, with the discharge capacity of 185.1 mAh g^{-1} and the charge capacity of 181.9 mAh g^{-1} at the current density of 1000 mA g^{-1}.

Therefore, the porous silicon can be created via these mental-assisted etching methods derived from the low-cost commercial microsized silicon bulks. Compared with the porous silicon obtained from silicon wafers, it can be found that the porous silicon prepared here have relative poor pore distribution and irregular porous structure. However, the low-cost endows this way with more attraction from the industry.

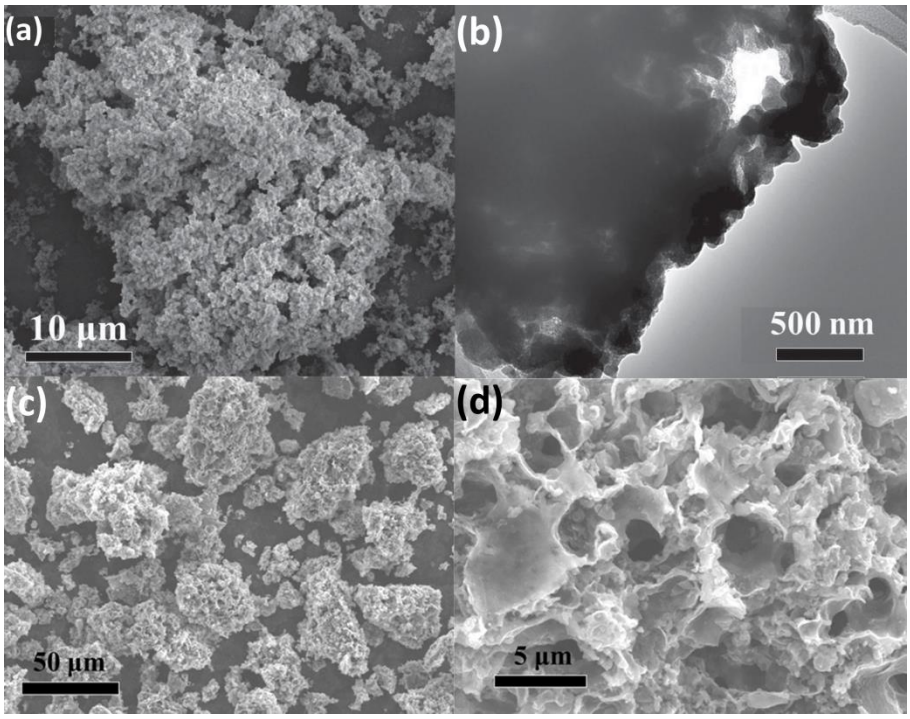

Figure 2. (a) SEM and (b) transmission electron microscope (TEM) images of porous silicon microparticles produced via an Fe-assisted chemical etching method.[59] Copyright 2015, Wiley-VCH Verlag GmbH and Co. KGaA, Weinheim. (c and d) SEM images of porous silicon microparticles produced via a Cu-assisted chemical etching method, Copyright 2014, Wiley-VCH Verlag GmbH and Co. KGaA, Weinheim.

2.2 Silica

Silica nanoparticles occupy a prominent position in scientific research, because of their easy preparation and their wide uses in various industrial applications. Silica has been demonstrated to be a high capacity anode material without further reduction to silicon, with a reversible capacity of 800 mAh g^{-1} over 200 cycles. Silica can be converted into silicon, however, through a facile magnesiothermic reduction, which makes it more attractive due to the high specific capacity of silicon. Silicon will be formed through the following reaction:

$$2Mg + SiO_2 \rightarrow 2MgO + Si \quad (3)$$

The magnesiothermic reduction method has three advantages. Firstly, the original structure of the

silica can be well maintained even after the reduction process. Secondly, a highly interconnected porous structure is created due to the etching of the MgO inclusions inside the sample during the magnesiothermic reduction.[60] Thirdly, the low processing temperature and short reaction time make this method more attractive than alternative methods.[61]

2.2.1 Natural Plants

As we all know, various kinds of plants in Nature are silica-enriched, because plants can absorb silica in the form of silicic acid ($Si(OH)_4$ or $Si(OH)_3O^-$) from the soil.[62] As a result, silica derivation from natural resources, especially from rice husks, is much more sustainable and lower cost than alternative methods, and also is attracting considerable research attention.[63-66] Recently, many researchers employed natural sources as the silica precursors, and then converted such kinds of nature-derived silica to silicon for energy storage applications. Cui's group prepared pure silica directly from rice husks and converted these silica particles to SiNPs with a conversion yield as high as 5% by mass (Figure 3a and 3b).[64] It was found that these recovered SiNPs exhibit high performances as LIB anodes, with high reversible capacity (2,790 mAh g^{-1}) and long cycle life (86% capacity retention over 300 cycles). Similarly to Cui's report, Jung et al. also employed rice husks as the precursor via the same process to prepare silicon-based anodes.[66] Silicon-based anodes with an ideal porous structure and much improved electrochemical performances were successfully obtained.

Apart from the rice husks, other kinds of the plant families, such as poaceae, equisetaceae, and cyperaceae are also promising choices.[67,68] For example, Yu *et al*. used reed leaves as the silica precursor to prepare the porous silica, and three-dimensional (3D) interconnected porous silicon was then synthesized via a magnesiothermic method (Figure 3c and 3d).[60] Nitrogen adsorption (Brunauer–Emmett–Teller, BET) measurements indicated that the initial 3D mesoporous silica

precursor had a BET surface area of 101 $m^2 g^{-1}$ and a total pore volume of 0.22 $cm^3 g^{-1}$. More importantly, even after the magnesiothermic reduction and the final carbon coating process, the prepared silicon anode still retained the original skeleton morphology of the reed leaves, which means good structural and thermal stability for this material. Owing to the excellent porous structure, an electrode capacity of about 420 mAh g^{-1} was still retained even after 4000 cycles at a current density of 10 C.

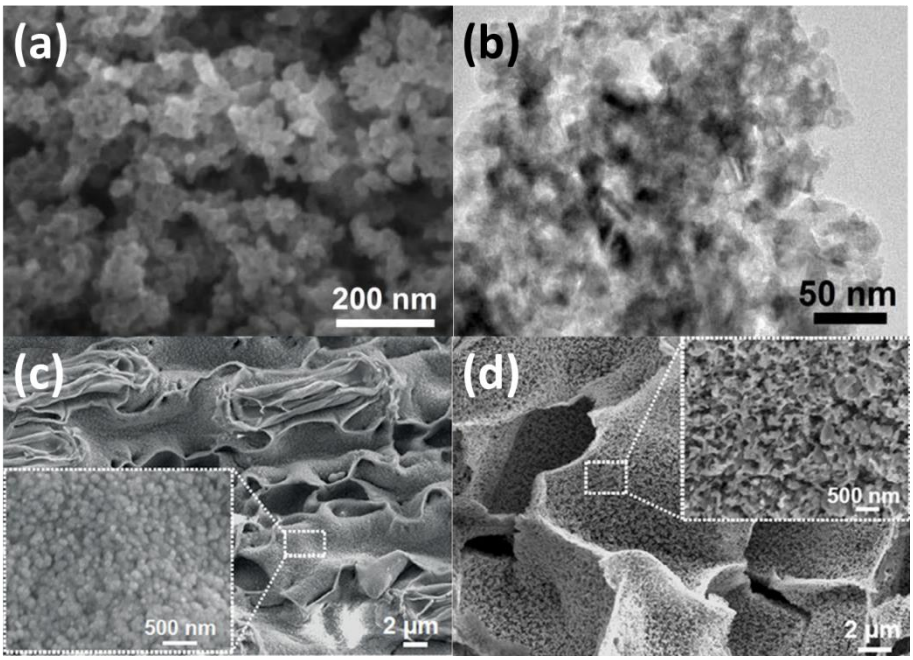

Figure 3. (a) SEM and (b) TEM images of silicon nanoparticles obtained by magnesiothermic reduction of silica derived from rice husks.[64] Copyright 2013, Nature Publishing Group. (c) SEM image of silica precursor converted from natural reed leaves, with the inset showing higher magnification, and (d) the finally achieved highly porous 3D silicon nanostructured anode for LIBs (inset is a high-magnification SEM image).[60] Copyright 2015, Wiley-VCH Verlag GmbH and Co. KGaA, Weinheim.

2.2.2 Sand

Recently, there have been some reports about using beach sand as the silica source for producing silicon anodes for LIBs.[69] Compared with the silicon derived from plants, only SiNPs

were finally obtained because the bulk structure of sea sand.[60] Favors et al. employed beach sand as the silica precursor to produce silicon-based anode materials via a magnesiothermic reduction method (Figure 4a and 4b).[70] The as-prepared sample has high phase purity and good crystallinity. The authors discovered that a three-dimensional (3D) network of nano-silicon was synthesized, and these SiNPs after carbon coating achieved a remarkable electrochemical performance, with a capacity of 1024 mAh g^{-1} at 2 A g^{-1} after 1000 cycles (Figure 4c). Also, in the same year, Kim et al, synthesized silicon nanosheets from natural sand by the s magnesiothermic reduction method (Figure 4d and 4e).[69] As reported, an Mg_2Si intermediate phase was formed at an early stage of the reduction process, leading to a two-dimensional (2D) silicon nanostructure. The thus-prepared silicon nanosheets have a leaf-like sheet morphology, ranging from several tens to several hundreds of nanometers in size, and show comparable electrochemical properties to commercial SiNPs as an anode for LIBs. In addition, in order to improve the electrochemical performance, reduced graphene oxide (RGO) was introduced to form a composite with these silicon nanosheets, leading to RGO-encapsulated silicon nanosheet electrodes. It was found that the RGO-encapsulated silicon-based anodes exhibited very high-reversible capacity and excellent rate capability.

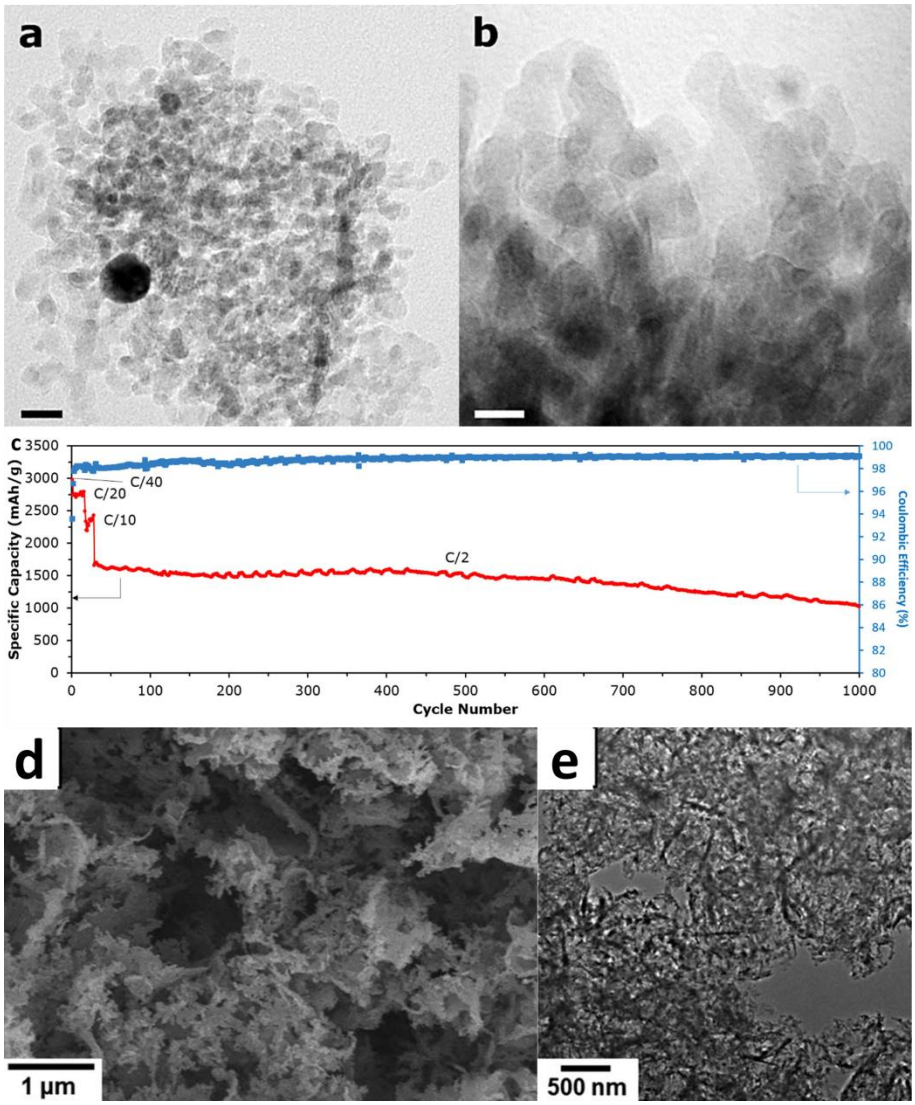

Figure 4. (a and b) TEM images and (c) cycling data at selected C-rates (1 C = 4A g^{-1}) for silicon nanoparticles.[70] Copyright 2014, Nature Publishing Group. (d) SEM and (e) TEM images of the as-synthesized silicon nanosheets obtained by magnesiothermic reduction of silica derived from sand.[69] Copyright 2014, Royal Society of Chemistry.

2.2.3 Tetraethyl Orthosilicate (TEOS)

Apart from the natural silica precursors, man-made silica has also attracted significant attention, especially the silica derived from TEOS, due to its ability to produce silica nanoparticles via the Stöber method.[71] This process works particularly well for particles with sizes of 30–60 nm, yielding silica spheres with excellent monodispersity. The large-sized silica, however, especially over 30 nm,

can lead to silicon nanoparticles with the same large size, which can limit the diffusion of the electrolyte, resulting in low capacity and coulombic efficiency. Therefore, Zhao's group synthesized mesoporous-silicon-based nanocomposites with ultra-small SiNPs uniformly embedded in a rigid mesoporous carbon framework, which was followed by the magnesiothermic reduction approach via a modified Stöber method (Figure 5a and 5b).[72] The silica used in this work was derived from the hydrolysis of TEOS. The authors found that the obtained mesoporous Si/C nanocomposites exhibit excellent performance, with a high reversible capacity of 1790 mAh g^{-1}, excellent coulombic efficiency (99.5%) and rate capability, and outstanding cycling stability (with the capacity remaining as high as 1480 mAh g^{-1} after 1000 cycles at a high current density of 2 A g^{-1}, Figure 5c).

Besides the silicon particles, some interesting structures can also be obtained in silicon via the reduction process from specific structured silica. For example, Yang et al. reported that a 3D mesoporous silicon material with a lotus-root-like morphology was successfully prepared by using mesoporous silica as the silicon precursor via a magnesiothermic reduction method (Figure 5d).[73] After surface carbon coating by a chemical vapor deposition (CVD) process, the obtained carbon covered silicon composite displayed a stable capacity of ~ 1500 mAh g^{-1} for 100 cycles at 1 C and high rate capability up to 15 C.

Compared with the man-made silicon, silicon derived from natural resources has some advantages, such as its abundance and low cost. In addition, the natural silica-enriched resources are already endowed with various structures in a very favorable nanoscale/microscale arrangement, with various morphologies ranging from sheets, to porous materials, to particles. These characteristics mean that natural silica precursors are more available for scalable fabrication and facile architectural design. On the other hand, natural precursors are not as pure as the man-made

silica, because some impurities are also present inside these resources, leading to the need for extra processes to remove the impurities, and increased cost and complexity. From this point of view, the man-made silica precursors are highly purified and size-controllable, which is very important for LIBs.

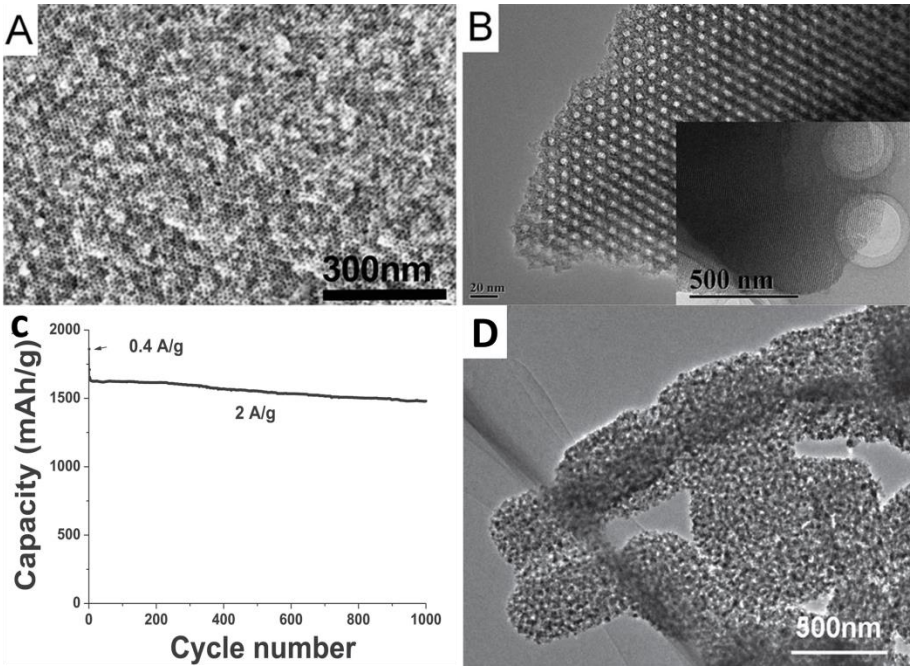

Figure 5. (a and b) TEM images and (c) the discharge capacity of mesoporous-silicon-based anode over 1000 cycles at a cycling rate of 2 A g^{-1} (with the current density for the first cycle 0.4 A g^{-1}).[72] Copyright 2014, Wiley-VCH Verlag GmbH and Co. KGaA, Weinheim. (d) TEM image of the lotus-root-like silicon anode obtained by magnesiothermic reduction of man-made silica.[73] Copyright 2011, Wiley-VCH Verlag GmbH and Co. KGaA, Weinheim.

2.3 Gaseous silicon-based sources

Up to the present, vapor-liquid-solid (VLS) growth, which was first proposed by Wagner and Ellis in the mid-1960s, has been the key mechanism for silicon-wire growth, based on using a silicon-bearing gas precursor in a chemical vapor deposition (CVD) reactor.[49,74-76] The temperatures used in this VLS-CVD process range from 300 up to well above 1000 ^{o}C, depending on the types of gas precursors and metal catalysts that are employed.[49,52] The gaseous silicon-bearing precursors,

such as silane (SiH_4), disilane (Si_2H_6), dichlorosilane (SiH_2Cl_2), and tetrachlorosilane ($SiCl_4$), are always employed as the silicon sources for synthesizing silicon nanowires, and gold (Au) is the most popular metallic catalyst for the VLS growth of nanosized silicon.[77-81] The name "VLS mechanism" refers, of course, to the fact that silicon from the vapor passes through a liquid droplet and finally ends up as a solid.[75] Briefly, this process involves the following stages: 1) formation of the liquid droplets of the metal-silicon alloy on the surface of the substrate; 2) the dissolution and diffusion of gaseous-silicon-based precursor into the silicon-Au alloy droplets; and 3) silicon precipitation and axial crystal growth due to supersaturation and nucleation at the liquid/ solid interface.[82]

2.3.1 SiH_4

SiH_4 is a very common and also very important silicon precursor in nanosized silicon preparation. During the VLS reaction, the silane decomposes, releasing silicon atoms which alloy with the metal, inducing eutectic formation, followed by silicon precipitation and nanowire growth from the silicon saturated nanoparticles.[52] For example, Chen's group[26] used SiH_4 as the silicon precursor along with a templating method to synthesize hollow silicon using the CVD process (Figure 6a and 6b). They found that a silicon shell could be created on the outer surface of the templates and showed a uniform thickness distribution. Meanwhile, the morphology of the hollow silicon is tunable by changing the structure of the templates, from hollow cubes, hollow spheres, and tubes, to flower-like hollow silicon. In particular, the flower-like silicon anode delivered a capacity of 814 mAh g^{-1} at a current density of 4.8 A g^{-1}, and retained 651 mAh g^{-1} after 700 cycles. Magasinski *et al.*[83] prepared a silicon-based anode material by coating carbon black with silicon via the CVD process, using SiH_4 as the silicon source. A silicon inverse opal structure could be prepared by filling a SiO_2 opal with silicon through CVD, using Si_2H_6 as the gas precursor,

followed by treatment in HF solution.[84] The thus-prepared amorphous silicon demonstrated promising cycling characteristics.

2.3.2 Si_2H_6

Another attractive precursor is Si_2H_6, which is more reactive than SiH_4. As a result, compared with SiH_4, the growth of silicon nanowires can be obtained at much lower pressures, which is very important for low-cost preparation. Thin-film amorphous silicon anodes were fabricated by low pressure chemical vapor deposition (LPCVD) using Si_2H_6 as a source gas by Jung and coworkers.[85] The prepared sample exhibited the very high reversible capacity of 4000 mAh g^{-1}, which is about 95% of the theoretical capacity of silicon. Unfortunately, the capacity fade was rapid after only 40 cycles. On the other hand, by reducing the current density to 400 mAh g^{-1} in each cycle, the cyclability could be enhanced to 1500 cycles.

2.3.3 SiH_xCl_y

Compared with SiH_4 and Si_2H_6, replacing the hydrogen atoms by chlorine, as in SiH_2Cl_2 and $SiCl_4$, can result in some drawbacks. The first is that the use of a chlorinated silane as the silicon precursor in the presence of hydrogen will lead to the generation of hydrochloric acid (HCl) during the CVD processing. Some undesirable etching of the substrate, the nanowires, and the facilities could be caused.[49] The second one is that the chlorinated silanes are more chemically stable than the non-chlorinated ones, leading to the need for a higher temperature to synthesize the nanosized silicon wires.[49] For example, the growth temperatures for $SiCl_4$ typically range from around 800–1000 ^oC, but only 400–600 °C for silane. The fabrication of nanosized silicon wires derived from SiH_2Cl_2 and $SiCl_4$ also has some advantages, however, and the main one is that we can have a much broader choice of possible VLS catalyst materials due the higher reaction temperature. For example, Pt,[86-88] Ni,[89] and Zn[90] are also very good choices if the VLS-CVD process is employed under even

higher temperatures. Mallet et al.[91] synthesized amorphous nanosized silicon wires by using $SiCl_4$ dissolved in an ionic liquid (1-butyl-1-methylpyrrolidinium bis(triuoromethanesulfonyl) imide (P1,4)) through the CVD process under a higher temperature. Yang's team prepared high-quality vertically aligned silicon nanowires using $SiCl_4$ as the silicon precursor in the VLS-CVD process (Figure 6c).[92] The thus-prepared silicon nanowires were grown vertically aligned with respect to the substrate, and the size distribution could be controlled by manipulating the colloid deposition on the substrate.

2.3.4 Silicon monoxide (SiO)

Another cost-effective way to synthesize nanosized silicon wires on a large scale is to evaporate solid SiO in a CVD reactor in a two-zone tube furnace.[75] The temperature for this method ranges from 900 to 1350 ^oC. SiO is first evaporated in the hotter zone which is placed at the end of the tube, and it then mixes with the inert gas stream and flows to the cooler part, where the gaseous SiO undergoes a disproportionation reaction into silicon and silica, thereby forming the final nanowires.[75,93] By carrying out the growth process over several hours, the obtained silicon nanowires with amorphous shells (up to several tens of nanometers in thickness) can reach millimeter lengths with varying diameters from about 5 to 100 nm.[94-96] Unfortunately, there are no reports on silicon anodes for LIBs obtained from SiO via this method.

2.3.5 Organic silicon sources

In addition, some organic silicon-based materials such as dimethyl dichlorosilane ($(CH_3)_2Cl_2Si$, DMDCS) can also be used as the silicon precursor via the CVD technique. Su's group[97] prepared silicon-based anode materials from this organosilane, which is widely used in industry, through a CVD process with DMDCS as the gaseous silicon precursor (Figure 6d). It was found that the silicon synthesized in this work had a club-like structure and was embedded on the surface of the

carbon substrate. The thus-prepared composite displayed a specific capacity of 562.0 mAh g^{-1} at a current density of 50 mA g^{-1}, much higher than that of commercial graphite anode.

In summary, silicon-based materials with various structures, such as hollow cubes, hollow spheres, nanowires and nanorods, have been successfully synthesized from these different silicon-containing gases. In addition, silicon-containing precursors are also playing a very important role not only in the lab research but also in the commercial silicon production. Due to the good penetrability of the gaseous precursors, perfect structures can be created via the templating method along with the assistance from templates.

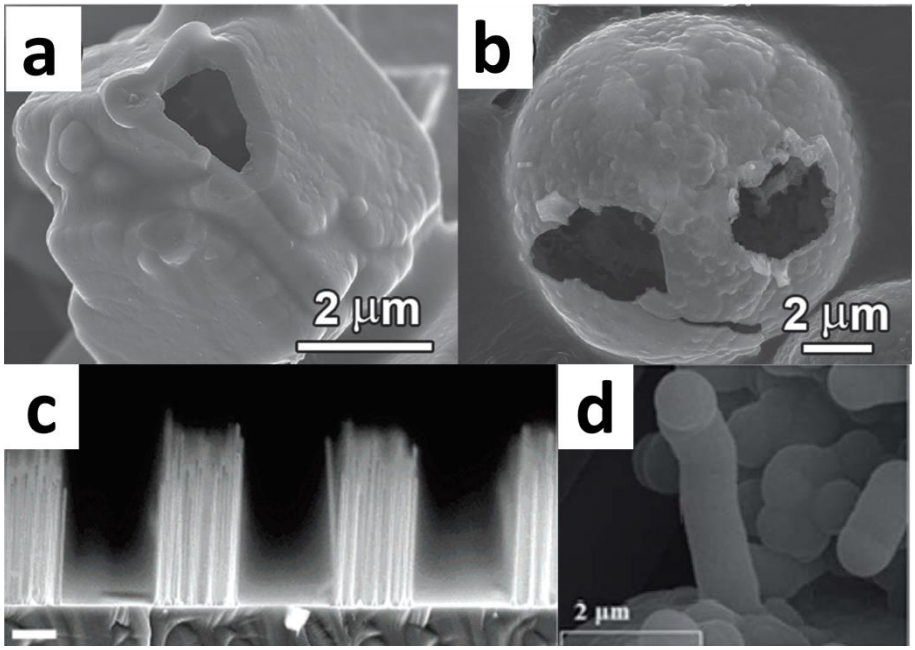

Figure 6. SEM images of hollow silicon derived from SiH_4 using two different carbonates as templates: hollow cubes (a) and hollow spheres (b).[26] Copyright 2014, Wiley-VCH Verlag GmbH and Co. KGaA, Weinheim. (c) Cross-sectional SEM image of silicon nanowires derived from $SiCl_4$.[92] Copyright 2005, American Chemical Society. and (d) SEM image of silicon-based rods synthesized from the organic silicon compound $(CH_3)_2Cl_2Si$.[97] Copyright 2013, The Royal Society of Chemistry.

2.4 Liquid silicon sources

Although the VLS process is a very promising method for thefabrication of nanowires, growth by this method thus far is limited, in that it is difficult to synthesize large quantities of nanowire materials on the substrate (only ∼200−250 μg cm^{-2} or ∼0.75 mg h^{-1}).[76,98,99] Furthermore, the silicon nanowires must be separated from the substrate using extra processes such as ultrasonication, which is destructive for retaining the morphology of the silicon nanowires. Therefore, some solution-based analogues of the VLS method have been developed using the supercritical fluid−liquid−solid (SFLS) growth technique.[100-103] Some liquid silicon sources have been successfully employed in this SFLS method for the preparation of carbon-coated silicon nanowires, such as trisilane,[102] phenylsilane,[98] monophenylsilane,[104] and diphenylsilane.[100]

For instance, Korgel's group[100] used diphenylsilane [$SiH_2(C_6H_5)_2$] as the silicon precursor, which was mixed with hexane and sterically stabilized gold nanoparticles at pressures of 200-270 bar at 500 °C within a reaction vessel. Another very attractive approach for the production of nanowires has been reported by Heitsch's team (Figure 7a to 7d).[102] They demonstrated the Au- and Bi-catalyzed growth of silicon nanowires in solution at atmospheric pressure using trisilane, Si_3H_8, as the silicon precursor. As reported by Cui's group,[98] composite electrodes composed of silicon nanowires were synthesized using phenylsilane as the silicon source via the SFLS method and mixed with amorphous carbon or carbon nanotubes before being evaluated in LIBs (Figure 7e and 7f). It was found that the silicon-based anode containing multiwalled carbon nanotubes as the conducting additive featured a reversible capacity of 1500 mAh g^{-1} for 30 cycles.

The main advantages of using liquid silicon sources for nanosized silicon wire fabrication are that very thin nanowires with good crystalline quality can be obtained in large amounts using a relatively simple equipment.[49] Compared with other synthesis methods which employ gaseous silicon as the precursor, the yield from this method is excellent. Nevertheless, controlled, in-place,

epitaxial growth of silicon nanowires can hardly be realized through this process.

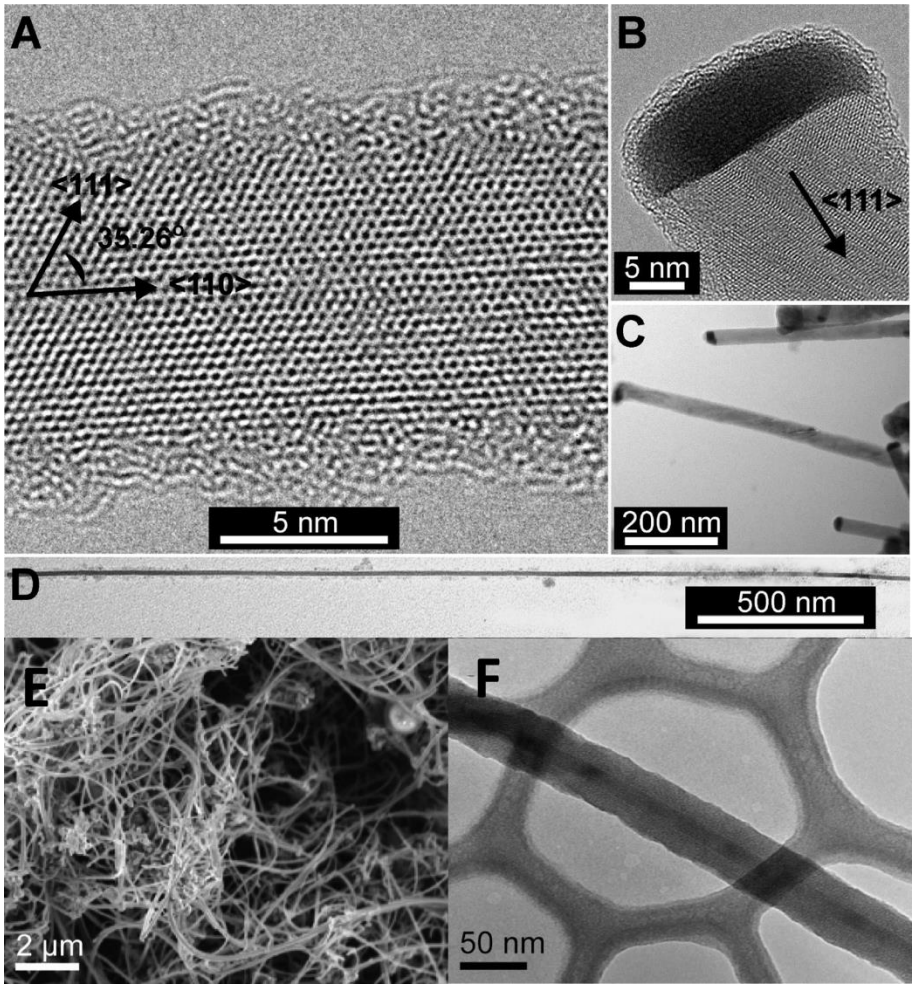

Figure 7. TEM images of Si nanowires synthesized in hot octacosane under ambient pressure by Si_3H_8 decomposition in the presence of either Au or Bi nanocrystals: (A) A Si nanowire synthesized at 410 °C with Au nanocrystal seeds; (B) a silicon nanowire with an Au seed at the tip; (C) Si nanowires grown using Bi nanocrystals as seeds (with energy dispersive spectroscopy (EDS) confirming that the dark particles at the tips of the wires are composed of Bi, providing evidence that the nanowires grow by the VLS mechanism); (D) a silicon nanowire (Bi seeded) longer than 3 μm.[102] Copyright 2008, American Chemical Society. (E) SEM and (F) TEM images of silicon nanowires derived from phenylsilane.[98] Copyright 2010, American Chemical Society.

2.5 Elemental silicon

Instead of a silicon chemical compound, elemental silicon has also attracted considerable

attention as the silicon precursor to prepare nanosized silicon via molecular beam epitaxy (MBE).[105-109] Silicon atoms, created by evaporating a heated high-purity solid Si source, are deposited onto the surface of a catalyst (Au) covered substrate, typically Si⟨111⟩. In this technique, elemental silicon, instead of a Si chemical compound, serves as the precursor for the fabrication of silicon nanowires. In MBE, there are two different Si fluxes governing wire growth. One is the direct flux of silicon from the pure silicon source; and the second one is the flux of diffusing Si adatoms from the silicon substrate surface.[75] The nanowires produced in this way are endowed with some advantages: (1) the Si nanowires grown in this way are epitaxial and oriented, following the ⟨111⟩ orientation; and (2) this technique can provide good controllability in terms of the incoming flux, which means that the doped wires can be grown by switching between evaporation sources.[75] The diameters of the Si nanowires cannot be precisely controlled, however, and only nanowires with diameters over 40 nm could be obtained.[105,106,109,110] In addition, the nanowire growth velocity is very low. Based on the recent reports, the growth velocity is just a few nanometers per minute.

In order to compare the electrochemical performances of silicon-based anodes derived from different kinds of precursors, we would like to provide a summary in Table 1 for further understanding.

Table 1 Electrochemical performance of the different Si-containing precursors derived Si-based anodes

Materials	**Precursor**	**Structure**	**Performance**	**Rates**	**Ref.**
Si	Silicon wafer	Porous Nanowire	1100 mAh g^{-1}	2 A g^{-1}	54
Si	Silicon wafer	Porous	3000 mAh g^{-1}	0.1 μA cm^{-2}	58
Si/C	Silicon bulks	Porous	1776 mAh g^{-1}	0.05 A g^{-1}	59

Si/C	Silicon microparticles	Porous	1036 mAh g^{-1}	0.05 A g^{-1}	40
Si	Rice husks	Nanoparticle	2200 mAh g^{-1}	0.84 A g^{-1}	64
Si	Rice husks	Nanoparticle	1554 mAh g^{-1}	2 A g^{-1}	66
Si/C	Reed leaves	Porous	1100 mAh g^{-1}	2 A g^{-1}	60
Si/C	Beach sand	Nanoparticle	1024 mAh g^{-1}	2 A g^{-1}	70
Si/RGO	Beach sand	Nanoparticle	1113 mAh g^{-1}	3 A g^{-1}	69
Si/C	SiO_2	Mesoporous	1480 mAh g^{-1}	2 A g^{-1}	72
Si/C	SiO_2	Lotus-root-like	1500 mAh g^{-1}	4 A g^{-1}	73
Si	SiH_4	Hollow flower-like	814 mAh g^{-1}	4.8 A g^{-1}	26
Si	Si_2H_6	Film	4000 mAh g^{-1}	100 μA cm^{-2}	85
Si/C	$(CH_3)_2Cl_2Si$	Nanorode	562.0 mAh g^{-1}	0.05 A g^{-1}	97
Si/C	C_6H_8Si	Nanowire	1500 mAh g^{-1}	0.65 A g^{-1}	98

4. Summary and open questions

To summarize, we have reviewed the recent advances in using various silicon precursors for the preparation of porous silicon and nanosized silicon for LIBs. Nanosized and porous Si-based anodes have been demonstrated to be promising for the emerging energy-related applications. Great efforts have been devoted to investigating LIBs based on Si-based anode materials in recent years, taking advantages of its high specific capacity, abundance, and environmental benignity, and overcoming its large volume expansion by the introduction of porous and nanosized structures. Despite many significant achievements, various difficult challenges still remain and need addressing to prepare high-performance silicon anodes with well-defined architectures from suitable Si precursors.

Porous or nanosized Si materials have shown great potential as LIB anodes, because the

introduced porous and nanosized structures can accommodate stress for reversible lithiation and delithiation, and rapid charge/discharge rates. Structure-regulated silicon nanowires can be produced from silicon wafers via an electroless/electrochemical etching process, or from gaseous silicon precursors, such as silane, disilane, dichlorosilane, and tetrachlorosilane through a vapor-liquid-solid method. The scaling-up of silicon-wafer-derived or gaseoussilicon -derived precursors, however, for silicon-based anodes may be relatively costly due to the low productivity and the high temperature needed for the process. Employing liquid Si precursors, such as trisilane, phenylsilane, monophenylsilane, and diphenylsilane, can lead to a large yield of silicon nanowires. In addition, the synthesis conditions in those methods are relatively mild. Unfortunately, the control of the nanowire distribution and dimensional growth regulation are poor. Producing silicon with specific structures from natural sources is also a popular way, but there are concerns with regard to the complex process required to purify the silica and also concerns about the different silica contents from various different natural-silica-enriched resources. Apart from the above-mentioned common silicon precursors, some special ones such as elemental silicon and SiO can also be treated as silicon sources via related techniques. These models need to be further developed, however, to allow for the influences of other factors, such as the growth conditions or the crystallography of the wire. This also holds true for the growth velocity of the wires. Among the different silicon precursors investigated so far, the preparation of silicon from man-made silica via a magnesiothermic reduction process seems to be most promising, but there is definitely a need for further investigations. A question in this context that is also unresolved is how to properly maintain the initial structure of the original silica precursors. Therefore, a better understanding of the magnesiothermic reduction mechanism would be highly desirable.

5. Acknowledgments

This work is supported by the the National High-tech R&D Program of China (863 Program, No. 2015AA034601) and Baosteel-Australia Joint Research & Development Centre (BAJC), Project BA14006, and Auto CRC 2020, Project 1-117. Lei Zhang would like to thank the China Scholarship Council (CSC) for his scholarship from China. The authors would like to also thank Dr. Tania Silver for critical reading of the manuscript.

References

1. **V. Etacheri, R. Marom, R. Elazari, G. Salitra and D. Aurbach, *Energy Environ. Sci.*, 2011, 4, 3243-3262.**
2. **A. Kraytsberg and Y. Ein-Eli, *Adv. Energy Mater.*, 2012, 2, 922-939.**
3. **X. Su, Q. L. Wu, J. C. Li, X. C. Xiao, A. Lott, W. Q. Lu, B. W. Sheldon and J. Wu, *Adv. Energy Mater.*, 2014, 4, 1300882.**
4. **H. Lee, M. Yanilmaz, O. Toprakci, K. Fu and X. W. Zhang, *Energy Environ. Sci.*, 2014, 7, 3857-3886.**
5. **Z. Ma, X. X. Yuan, L. Li, Z. F. Ma, D. P. Wilkinson, L. Zhang and J. J. Zhang, *Energy Environ. Sci.*, 2015, 8, 2144-2198.**
6. **X. L. Hu, W. Zhang, X. X. Liu, Y. N. Mei and Y. Huang, *Chem. Soc. Rev.*, 2015, 44, 2376-2404.**
7. **T. L. Kulova, *Russ. J. Electrochem.*, 2013, 49, 1-25.**
8. **V. Deimede and C. Elmasides, *Energy Technology*, 2015, 3, 453-468.**
9. **L. Zhang, M. Zhang, Y. Wang, Z. Zhang, G. Kan, C. Wang, Z. Zhong and F. Su, *J. Mater. Chem. A*, 2014, 2, 10161.**
10. **M. Yoshio, H. Wang, K. Fukuda, T. Umeno, T. Abe and Z. Ogumi, *J. Mater. Chem.*, 2004, 14, 1754.**
11. **C. K. M. Endo, K. Nishimura, T. Fujino, K. Miyashita, *Carbon*, 38, 183-197.**
12. **A. R. Kamali and D. J. Fray, *J. New Mater. Electrochem. Syst.*, 2010, 13, 147-160.**
13. **F. W. Yuan, H. J. Yang and H. Y. Tuan, *ACS Nano*, 2012, 6, 9932-9942.**
14. **D. T. Ngo, R. S. Kalubarme, H. T. T. Le, J. G. Fisher, C. N. Park, I. D. Kim and C. J. Park, *Adv. Funct. Mater.*, 2014, 24, 5291-5298.**
15. **T. Song, H. Y. Cheng, K. Town, H. Park, R. W. Black, S. Lee, W. I. Park, Y. G. Huang, J. A. Rogers, L. F. Nazar and U. Paik, *Adv. Funct. Mater.*, 2014, 24, 1458-1464.**
16. **T. Song, Y. Jeon, M. Samal, H. Han, H. Park, J. Ha, D. K. Yi, J. M. Choi, H. Chang, Y. M. Choi and U. Paik, *Energy Environ. Sci.*, 2012, 5, 9028-9033.**
17. **D. C. Lin, Z. D. Lu, P. C. Hsu, H. R. Lee, N. Liu, J. Zhao, H. T. Wang, C. Liu and Y. Cui, *Energy Environ. Sci.*, 2015, 8, 2371-2376.**
18. **N. Liu, H. Wu, M. T. McDowell, Y. Yao, C. Wang and Y. Cui, *Nano Lett.*, 2012, 12, 3315-21.**
19. **Z. L. Nian Liu, Jie Zhao, Matthew T. McDowell, Hyun-Wook Lee, Wenting Zhao and Yi Cui, *Nat. Nanotechnol.*, 2014, 9, 187-192.**
20. **G. Derrien, J. Hassoun, S. Panero and B. Scrosati, *Adv. Mater.*, 2007, 19, 2336.**
21. **Z. Q. Zhu, S. W. Wang, J. Du, Q. Jin, T. R. Zhang, F. Y. Cheng and J. Chen, *Nano Lett.*, 2014, 14, 153-157.**
22. **M. T. McDowell, S. W. Lee, W. D. Nix and Y. Cui, *Adv. Mater.*, 2013, 25, 4966-85.**

23. D. Ma, Z. Cao and A. Hu, *Nano Micro. Lett.*, 2014, 6, 347-358.

24. H. K. Liu, Z. P. Guo, J. Z. Wang and K. Konstantinov, *J. Mater. Chem.*, 2010, 20, 10055.

25. L. Zhang, Y. H. Wang, G. W. Kan, Z. L. Zhang, C. G. Wang, Z. Y. Zhong and F. B. Su, *RSC Adv.*, 2014, 4, 43114-43120.

26. X. Huang, J. Yang, S. Mao, J. Chang, P. B. Hallac, C. R. Fell, B. Metz, J. Jiang, P. T. Hurley and J. Chen, *Adv. Mater.*, 2014, 26, 4326-32.

27. J. Luo, X. Zhao, J. Wu, H. D. Jang, H. H. Kung and J. Huang, *J. Phys. Chem. Lett.*, 2012, 3, 1824-9.

28. J.-H. Lee, W.-J. Kim, J.-Y. Kim, S.-H. Lim and S.-M. Lee, *J. Power Sources*, 2008, 176, 353-358.

29. H. Wu and Y. Cui, *Nano Today*, 2012, 7, 414-429.

30. M. Y. Ge, J. P. Rong, X. Fang and C. W. Zhou, *Nano Lett.*, 2012, 12, 2318-2323.

31. A. I. Hochbaum, D. Gargas, Y. J. Hwang and P. D. Yang, *Nano Lett.*, 2009, 9, 3550-3554.

32. F. Bai, M. C. Li, D. D. Song, H. Yu, B. Jiang and Y. F. Li, *J. Solid State Chem.*, 2012, 196, 596-600.

33. Y. Q. Qu, H. L. Zhou and X. F. Duan, *Nanoscale*, 2011, 3, 4060-4068.

34. N. Bachtouli, S. Aouida and B. Bessais, *Microporous Mesoporous Mater.*, 2014, 187, 82-85.

35. F. Bai, M. C. Li, D. D. Song, H. Yu, B. Jiang and Y. F. Li, *J. Solid State Chem.*, 2012, 196, 596-600.

36. S. Y. Li, W. H. Ma, Y. Zhou, X. H. Chen, Y. Y. Xiao, M. Y. Ma, W. J. Zhu and F. Wei, *Nanoscale Res. Lett.*, 2014, 9.

37. L. F. Liu and X. Q. Bao, *Mater. Lett.*, 2014, 125, 28-31.

38. O. Lotty, N. Petkov, Y. M. Georgiev and J. D. Holmes, *Jpn. J. Appl. Phys.*, 2012, 51, 11PE03.

39. Z. Zhang, Y. Wang, W. Ren, Q. Tan, Z. Zhong and F. Su, *Adv. Electron.Mater.*, 2015, 1, 1400059.

40. Z. Zhang, Y. Wang, W. Ren, Q. Tan, Y. Chen, H. Li, Z. Zhong and F. Su, *Angew. Chem. Int. Ed.*, 2014, 53, 5165-9.

41. J. S. Kim, H. G. Jung, W. Choi, H. Y. Lee, D. Byun and J. K. Lee, *Int. J. Hydrogen Energy*, 2014, 39, 21420-21428.

42. A. Ramizy, Z. Hassan and K. Omar, *J. Mater. Sci. - Mater. Electron.*, 2011, 22, 717-723.

43. K. Omar, Y. Al-Douri, A. Ramizy and Z. Hassan, *Superlattices Microstruct.*, 2011, 50, 119-127.

44. B. Kang, C. H. Jeong, C. Kim, M. Y. Kim, B. H. Choi, M. S. Lee and H. S. Kim, *J. Nanosci. Nanotechnol.*, 2015, 15, 5291-5294.

45. X. C. Li, B. K. Tay, G. F. You and Y. Yang, *Processing of 2008 2nd IEEE International Nanoelectronics Conference*, 2008, 1-3, 860-862.

46. Z. C. Li, L. Zhao, H. W. Diao, H. L. Li, C. L. Zhou and W. J. Wang, *J. Solid State Sci. Tech.*, 2013, 2, Q65-Q68.

47. Z. T. Qin, J. Joo, L. Gu and M. J. Sailor, *Part. Part. Syst. Char.*, 2014, 31, 252-256.

48. T. Schmidt, M. Zhang, S. Yu and J. Linnros, *Appl. Phys. Lett.*, 2014, 105.

49. J. V. W. V. Schmidt, and U. Gösele, *Chem. Rev.*, 2010, 110, 361-188.

50. Y. Qu, H. Zhou and X. Duan, *Nanoscale*, 2011, 3, 4060-8.

51. K. Q. Peng, Y. J. Yan, S. P. Gao and J. Zhu, *Adv. Mater.*, 2002, 14, 1164-1167.

52. M. R. Zamfir, H. T. Nguyen, E. Moyen, Y. H. Lee and D. Pribat, *J. Mater. Chem. A*, 2013, 1, 9566.

53. K. Q. Peng, J. J. Hu, Y. J. Yan, Y. Wu, H. Fang, Y. Xu, S. T. Lee and J. Zhu, *Adv. Funct. Mater.*, 2006, 16, 387-394.

54. M. Y. Ge, J. P. Rong, X. Fang and C. W. Zhou, *Nano Lett.*, 2012, 12, 2318-2323.

55. A. U. Jr., *At&T Tech. J.*, 1956, 35, 333-347.

56. M. Ge, X. Fang, J. Rong and C. Zhou, *Nanotechnology*, 2013, 24, 422001.

57. T. D. R, *J. Electrochem. Soc.*, 1958, 105, 55-56.

58. M. Thakur, M. Isaacson, S. L. Sinsabaugh, M. S. Wong and S. L. Biswal, *J. Power Sources*, 2012, 205,

426-432.

59. Z. L. Zhang, Y. H. Wang, W. F. Ren, Q. Q. Tan, Z. Y. Zhong and F. B. Su, *Adv. Electron. Mater.*, 2015, 1, 1400059.

60. J. Liu, P. Kopold, P. A. van Aken, J. Maier and Y. Yu, *Angew. Chem. Int. Ed.*, 2015, 54, 9632-9636.

61. F. H. Du, B. Li, W. Fu, Y. J. Xiong, K. X. Wang and J. S. Chen, *Adv. Mater.*, 2014, 26, 6145-+.

62. M. J. Hodson, P. J. White, A. Mead and M. R. Broadley, *Annals of Botany*, 2005, 96, 1027-1046.

63. L. Y. Sun and K. C. Gong, *Ind. Eng. Chem. Res.*, 2001, 40, 5861-5877.

64. N. Liu, K. Huo, M. T. McDowell, J. Zhao and Y. Cui, *Sci. Rep.*, 2013, 3, 1919.

65. D. P. Wong, R. Suriyaprabha, R. Yuvakumar, V. Rajendran, Y. T. Chen, B. J. Hwang, L. C. Chen and K. H. Chen, *J. Mater. Chem. A*, 2014, 2, 13437-13441.

66. D. S. Jung, M. H. Ryou, Y. J. Sung, S. B. Park and J. W. Choi, *P. Natl. Acad. of Sci. USA*, 2013, 110, 12229-12234.

67. H. A. Currie and C. C. Perry, *Annals of Botany*, 2007, 100, 1383-1389.

68. E. Epstein, *Ann. Appl. Biol.*, 2009, 155, 155-160.

69. W. S. Kim, Y. Hwa, J. H. Shin, M. Yang, H. J. Sohn and S. H. Hong, *Nanoscale*, 2014, 6, 4297-4302.

70. Z. Favors, W. Wang, H. H. Bay, Z. Mutlu, K. Ahmed, C. Liu, M. Ozkan and C. S. Ozkan, *Sci. Rep.*, 2014, 4, 5623.

71. E. Dingsoyr and A. A. Christy, *Surf. Colloid Sci.*, 2001, 116, 67-73.

72. R. Zhang, Y. Du, D. Li, D. Shen, J. Yang, Z. Guo, H. K. Liu, A. A. Elzatahry and D. Zhao, *Adv. Mater.*, 2014, 26, 6749-55.

73. H. P. Jia, P. F. Gao, J. Yang, J. L. Wang, Y. N. Nuli and Z. Yang, *Adv. Energy Mater.*, 2011, 1, 1036-1039.

74. Y. W. Wang, V. Schmidt, S. Senz and U. Gosele, *Nat. Nanotechnol.*, 2006, 1, 186-189.

75. V. Schmidt, J. V. Wittemann, S. Senz and U. Gosele, *Adv. Mater.*, 2009, 21, 2681-2702.

76. R. S. Wagner and W. C. Ellis, *Appl. Phys. Lett.*, 1964, 4, 89.

77. J. Westwater, D. P. Gosain, S. Tomiya, S. Usui and H. Ruda, *J. Vac. Sci. Technol., B*, 1997, 15, 554-557.

78. I. K. Ng, K. Y. Kok, S. S. Z. Abidin, N. U. Saidin, T. F. Choo, B. T. Goh, S. K. Chong and S. A. Rahman, *Mater. Res. Innovations*, 2011, 15, 55-58.

79. Y. Y. Su, X. P. Wei, F. Peng, Y. L. Zhong, Y. M. Lu, S. Su, T. T. Xu, S. T. Lee and Y. He, *Nano Lett.*, 2012, 12, 1845-1850.

80. T. Stelzner, G. Andra, E. Wendler, W. Wesch, R. Scholz, U. Gosele and S. Christiansen, *Nanotechnology*, 2006, 17, 2895-2898.

81. J. B. Hannon, S. Kodambaka, F. M. Ross and R. M. Tromp, *Nature*, 2006, 440, 69-71.

82. K.-Q. Peng, X. Wang, L. Li, Y. Hu and S.-T. Lee, *Nano Today*, 2013, 8, 75-97.

83. P. D. A. Magasinski, B. Hertzberg, A. Kvit, J. Ayala and G. Yushin, *Nat. Mater.*, 2010, 9, 353-358.

84. A. E. a. G. A. Ozin, *Adv. Funct. Mater.*, 2009, 19, 1999-2010.

85. H. Jung, M. Park, S. H. Han, H. Lim, S.-K. Joo, *Solid State Commun.*, 2003, 125, 387-390.

86. E. C. Garnett, W. J. Liang and P. D. Yang, *Adv. Mater.*, 2007, 19, 2946.

87. B. Z. Liu, Y. F. Wang, S. Dilts, T. S. Mayer and S. E. Mohney, *Nano Lett.*, 2007, 7, 818-824.

88. H. Jeong, T. E. Park, H. K. Seong, M. Kim, U. Kim and H. J. Choi, *Chem. Phys. Lett.*, 2009, 467, 331-334.

89. N. L. Wang, Y. J. Zhang and J. Zhu, *J. Mater. Sci. Lett.*, 2001, 20, 89-91.

90. H. F. Al-Taay, M. A. Mahdi, D. Parlevliet, Z. Hassan and P. Jennings, *Superlattices Microstruct.*, 2014, 68, 90-100.

91. J. Mallet, M. Molinari, F. Martineau, F. Delavoie, P. Fricoteaux and M. Troyon, *Nano Lett.*, 2008, 8, 3468-3474.

92. A. I. Hochbaum, R. Fan, R. R. He and P. D. Yang, *Nano Lett.*, 2005, 5, 457-460.

93. Z. W. Pan, Z. R. Dai, L. Xu, S. T. Lee and Z. L. Wang, *J. Phys. Chem. B*, 2001, 105, 2507-2514.

94. W. S. Shi, H. Y. Peng, Y. F. Zheng, N. Wang, N. G. Shang, Z. W. Pan, C. S. Lee and S. T. Lee, *Adv. Mater.*, 2000, 12, 1343-1345.

95. Y. Shi, Q. Hu, H. Araki, H. Suzuki, H. Gao, W. Yang and T. Noda, *Appl. Phys. Mater. Sci. Proc.*, 2005, 80, 1733-1736.

96. Y. F. Zhang, Y. H. Tang, C. Lam, N. Wang, C. S. Lee, I. Bello and S. T. Lee, *J. Cryst. Growth*, 2000, 212, 115-118.

97. X. Zhu, H. Chen, Y. Wang, L. Xia, Q. Tan, H. Li, Z. Zhong, F. Su and X. S. Zhao, *J. Mater. Chem. A*, 2013, 1, 4483.

98. C. K. Chan, R. N. Patel, M. J. O'Connell, B. A. Korgel and Y. Cui, *Acs Nano*, 2010, 4, 1443-1450.

99. A. M. Morales and C. M. Lieber, *Science*, 1998, 279, 208-211.

100. J. D. Holmes, K. P. Johnston, R. C. Doty and B. A. Korgel, *Science*, 2000, 287, 1471-1473.

101. T. Hanrath and B. A. Korgel, *Adv. Mater.*, 2003, 15, 437-440.

102. A. T. Heitsch, D. D. Fanfair, H. Y. Tuan and B. A. Korgel, *J. Am. Chem. Soc.*, 2008, 130, 5436-+.

103. H. Y. Tuan and B. A. Korgel, *Chem. Mater.*, 2008, 20, 1239-1241.

104. D. C. Lee, T. Hanrath and B. A. Korgel, *Angew. Chem. Int. Ed.*, 2005, 44, 3573-3577.

105. L. Schubert, P. Werner, N. D. Zakharov, G. Gerth, F. M. Kolb, L. Long, U. Gosele and T. Y. Tan, *Appl. Phys. Lett.*, 2004, 84, 4968-4970.

106. N. D. Zakharov, P. Werner, G. Gerth, L. Schubert, L. Sokolov and U. Gosele, *J. Cryst. Growth*, 2006, 290, 6-10.

107. N. Zakharov, P. Werner, L. Sokolov and U. Gosele, *Physica E*, 2007, 37, 148-152.

108. B. Fuhrmann, H. S. Leipner, H. R. Hoche, L. Schubert, P. Werner and U. Gosele, *Nano Lett.*, 2005, 5, 2524-2527.

109. P. Werner, N. D. Zakharov, G. Gerth, L. Schubert and U. Gosele, *Int. J. Mater. Res.*, 2006, 97, 1008-1015.

110. P. Das Kanungo, N. Zakharov, J. Bauer, O. Breitenstein, P. Werner and U. Goesele, *Appl. Phys. Lett.*, 2008, 92.